TRPV1 activation relies on hydration/dehydration of nonpolar cavities

Marina A. Kasimova[1], Aysenur Yazici[2], Yevgen Yudin[2], Daniele Granata[1], Michael L. Klein[1], Tibor Rohacs[2], Vincenzo Carnevale[1]

[1]*Institute for Computational Molecular Science, Temple University, Philadelphia, PA 19122*
[2]*Department of Pharmacology, Physiology and Neuroscience, Rutgers–New Jersey Medical School, Newark, NJ 07103*

Email: vincenzo.carnevale@temple.edu

SUPPLEMENTARY TEXT

Distance maps

To quantitatively compare the three cryo-EM structures, apo, capsaicin-bound (CAP-bound) and resiniferatoxin-bound (RTX)[1,2], we computed the distances between their S6 and S4-S5 residues (Figure S11). We found an increased distance (> 5 Å) between the C-terminal parts of S6 and S4-S5 in the CAP-bound state compared to the two others, in which the corresponding elements are in contact with each other (the distance is smaller than 5 Å). Therefore, a possible scenario for the apo/CAP-bound/RTX-bound transition is a sequential uncoupling (apo/CAP-bound) and recoupling (CAP-bound/RTX-bound) of the S6 C-terminus to the S4-S5 linker.

Using the MD trajectories of the TRPV1 conformations with hydrated and empty PCs, we explored whether their S6 segments remain uncoupled from the S4-S5 linkers as in the initial CAP-bound state. To do so, we estimated the distance maps for S4-S5 and S6 using the second halves of the two trajectories. We found that, in the channel with hydrated PCs, the two C-termini (of S6 and S4-S5) have only few contacting residues, a situation similar to the initial state that indicates uncoupling (Figure S11, S12). By contrast, in the channel with empty PCs, the two C-termini approach each other and establish multiple interactions, as in the apo or RTX-bound states (Figure S11, S12).

We observed the S6/S4-S5 uncoupling in all four subunits of the channel with hydrated PCs, as well as tight interaction between these elements in all four subunits of the channel with empty PCs; this indicates a critical dependence of the S6/S4-S5 conformation on the initial conditions, i.e. hydrating the PCs or leaving them empty.

Water in the peripheral cavities

The PCs are connected to the intracellular solution and run parallel to the central pore up to the middle of S6 (approximately). To estimate how far these cavities expand upward, we calculated water density along the normal to the membrane in the closed and open states. As a control case, we performed this analysis also for the apo structure. The water density profiles superimposed with those of the central pore are shown in Figure S13.

In the closed state, the water density in the PCs extends up to the level of the central cavity, while that in the central pore shows an interruption at the lower gate. This indicates that the S6 residues higher than I679 cannot be accessed by the intracellular solution through the central pore; however, some of them (up to those of the central cavity) can be accessed through the PCs. In the apo state, there is no water inside the central pore at the level of the lower gate, which confirms that the S6 residues, in particular those in the segment L672-I678, do not have direct communication with the intracellular solution through this compartment. Interestingly, in this state, the water density inside the PCs has a small, yet non zero value. Indeed, during the MD simulation, we observed occasional hydration of the PCs. These events, however, were rare, suggesting that the “hydrated PCs” conformation is significantly less stable than the dehydrated one. Finally, in the open state, the central pore is continuously hydrated, while the water density inside the PCs is interrupted at the lower gate, which indicates that S6 is accessible to the intracellular solution only through the central pore.

Evolutionary conserved polar character of S6

In our prposed activation mechanism, N676 plays a crucial role: when it faces the PCs, the central pore is only partially hydrated and hence non-conductive, while when it faces the central cavity, the central pore is continuously hydrated and thus conductive. Therefore, a peculiar pattern of amino acid polarity on S6 (all the residues hydrophobic except N676) and the ability of N676 to rotate in and out the central cavity underlie the TRPV1 activation mechanism. This raises immediately a question: Is this pattern of polarity evolutionarily conserved? If so, is it conserved across the entire family of TRP channels? To explore this possibility, we examined a large, comprehensive multiple sequence alignment[3] and estimated the average polarity of each S6 position (665-679, TRPV1 numbering)[4] (see Methods). The result of this analysis is shown in Figure S14.

While for most of the N-terminal part (from residue 665 to 671), the amino acid polarity shows large variability and varies from hydrophobic to hydrophilic, for the C-terminus part (from residue 672 to 678), it is remarkably invariant: all the residues are hydrophobic except for that at position 676, which is hydrophilic. This conservation is suggestive of a specific evolutionary pressure and might indicate that all TRP channels share the activation mechanism proposed in this work.

Temperature dependence of the central pore hydration

To test whether the hydration of the central pore is temperature dependent, we calculated the evolution of water density inside this compartment along the three metadynamics trajectories (Figure S15). Interestingly, we found that water density profiles differ at 340 K, and 300 K and 280 K. In particular, while at 300 K and 280 K the water density fluctuations occur only at the level of the central cavity, at 340 K they can reach the lower gate. We also noticed that water bursts in the central cavity are well correlated with the N676 dynamics at all the temperatures, providing further elements of support to our proposed activation mechanism in which the N676 orientation controls the hydration of the central pore. Furthermore, the gap in the water density observed at the level of the selectivity filter is less pronounced at 340 K than 300 K and 280 K. Based on these observations we conclude that the hydration of the central pore is significantly increased at high temperature.

Molecular origin of temperature dependent gating and estimate of Q_{10}

Here we discuss how ΔG can show a non-trivial dependence on temperature when the heat capacity is not constant across a conformational transition and how to predict ΔG as a function of temperature under these circumstances. Let us start by considering how the enthalpy H and the entropy S vary with temperature:

$$dH(T,p) = \left(\frac{\partial H}{\partial T}\right)_p dT + \left(\frac{\partial H}{\partial p}\right)_T dp;$$
$$dS(T,p) = \left(\frac{\partial S}{\partial T}\right)_p dT + \left(\frac{\partial S}{\partial p}\right)_T dp,$$

which at constant pressure become:

$$dH(T,p) = \left(\frac{\partial H}{\partial T}\right)_p dT; \quad dS(T,p) = \left(\frac{\partial S}{\partial T}\right)_p dT.$$

To identify these two partial derivatives with thermodynamic observables, we can use the first and second principles. Thus the derivative of the entropy with respect to

temperature can be expressed as a function of the heat capacity at constant pressure, C_p:

$$dS = \frac{\delta Q}{T} = \frac{C_p\ dT}{T};$$

therefore

$$\left(\frac{\partial S}{\partial T}\right)_p = \frac{C_p}{T}.$$

Likewise, the derivative of the enthalpy can be found using the first principle (at constant pressure):

$$\delta Q = dH - \cancel{V dp} = C_p\ dT$$

that implies

$$\left(\frac{\partial H}{\partial T}\right)_p = C_p\,.$$

To describe the temperature dependence of Gibbs free energy G, we will first Taylor expand H and S around temperature T to second order in the increment ΔT and then calculate the free energy as $G=H-TS$. Accordingly,

$$\begin{aligned}
H(T+\Delta T) &= H(T) + \left(\frac{\partial H}{\partial T}\right)_p \Delta T + \frac{1}{2}\left(\frac{\partial^2 H}{\partial T^2}\right)_p \Delta T^2 + O(\Delta T^3) = \\
&= H(T) + C_p\ \Delta T + \frac{1}{2}\frac{\partial C_p}{\partial T}\Delta T^2 + O(\Delta T^3); \\
S(T+\Delta T) &= S(T) + \left(\frac{\partial S}{\partial T}\right)_p \Delta T + \frac{1}{2}\left(\frac{\partial^2 S}{\partial T^2}\right)_p \Delta T^2 + O(\Delta T^3) = \\
&= S(T) + \frac{C_p}{T}\ \Delta T + \frac{1}{2T}\frac{\partial C_p}{\partial T}\Delta T^2 - \frac{1}{2}\frac{C_p}{T^2}\Delta T^2 + O(\Delta T^3).
\end{aligned}$$

Neglecting terms of order ΔT^3 or higher, Gibbs free energy reads:

$$\begin{aligned}
G(T+\Delta T) &= H(T+\Delta T) - (T+\Delta T)S(T+\Delta T) \approx \\
&\approx H(T) + C_p\Delta T + \frac{1}{2}\frac{\partial C_p}{\partial T}\Delta T^2 - (T+\Delta T)\left[S(T) + \right. \\
&\left. + \frac{C_p}{T}\Delta T + \frac{1}{2T}\frac{\partial C_p}{\partial T}\Delta T^2 - \frac{1}{2}\frac{C_p}{T^2}\Delta T^2\right] \approx \\
&\approx G(T) - S(T)\Delta T - \frac{1}{2}\frac{C_p}{T}\Delta T^2.
\end{aligned}$$

The free energy shows an expected linear dependence on temperature due to the entropy term plus an additional quadratic term. Let us consider the open and closed states of the ion channel; the free energy difference reads:

$$\begin{aligned}\Delta G(T+\Delta T) &= G^o(T+\Delta T) - G^c(T+\Delta T) = \\ &= G^o(T) - G^c(T) - S^o(T)\Delta T + S^c(T)\Delta T + \\ &- \frac{C_p^o(T)}{2T}\Delta T^2 + \frac{C_p^c(T)}{2T}\Delta T^2 = \\ &= \Delta G(T) - \Delta S(T)\Delta T - \frac{1}{2}\frac{\Delta C_p(T)}{T}\Delta T^2.\end{aligned} \quad (1)$$

Therefore, if the two thermodynamic states (open and closed) have different heat capacities then the free energy difference depends quadratically on temperature. In particular, if the heat capacity of the open state is larger than that of the closed one, an increase in temperature will alter the conformational equilibrium, favoring the former and disfavoring the latter (i.e. "activating" the channel). Can the open state show a larger heat capacity compared to the closed one? If so, what are the possible physical underpinnings of this difference? It has been suggested[5,6] that a change in the hydrophobic surface area exposed to the solvent between the open and closed state provides a justification for a large ΔC_p. Given the wet/dry transitions observed in our simulations, we provide independent support to this notion that hydrophobic interactions are key to temperature dependence of activation. However, we consider here a slightly different mechanism to rationalize the origin of a large positive ΔC_p.

We start by noting that the heat capacity is in its own right a function of temperature; therefore ΔC_p can, in principle, be non-zero only for specific values of temperature. This would be true, for instance, if the open state underwent a first order phase transition. In this case a (formally) divergent heat capacity would give rise to exceptionally large values of C_p and thus ΔC_p. It is intriguing that the wet/dry transition that we observe in the nonpolar cavities of the open state is the microscopic-length-scale analogue of a first order phase transition, namely the liquid-vapor transition. Indeed, the free energy profiles along the order parameter (the hydration number) indicate that at 280 and 300 K the probability distribution is approximately Gaussian and fluctuations are relatively small. By contrast, at 340 K the free energy profile "flattens out" and the cavity can host, with approximately equal probability, zero, one, or more water molecules. The resulting water density fluctuations are the signature of criticality and reflect a sharp increase of the number of accessible degrees of freedom, a fact that is, in turn, responsible for a sudden increase of the heat capacity. The idea that the wet/dry transition produces a "hump" in the plot of C_p vs T has been confirmed in several studies focused on the thermodynamic properties of water confined in small non-polar cavities of size comparable to the protein pockets studied here. In particular, these waters adopt the configurations observed in gas-phase clusters[7,8] and it has been shown[9] that theri melting can produce spikes in the heat capacity as large as 20 kcal/mol/K. Taking this number at face value, the term of ΔG proportional to ΔT^2 could be negative and as large

as ~13 kcal/mol (at 310 K and for a ΔT of 10 K), a remarkable stabilization of the open state that would be likely able to activate the channel. We note that such mechanism does not rely on large conformational rearrangements of the channel (like the ones necessarily required to account for a big change in the hydrophobic solvent accessible area) and thus is consistent with the structures of the open and closed states inferred by cryo-electron microscopy.

In closing, to make a direct connection with experiments, we calculated the temperature coefficient Q_{10} and found it in good agreement with what found by Jara-Oseguera et al[10]. To this end, we used the estimated ΔG at the three different values of temperature (280, 300 and 340 K) to calculate the coefficients of the quadratic form in (1). Q_{10} was then calculated as the ratio between the open probabilities P_0 at temperatures $T+10$ and T:

$$Q_{10}(T) = \frac{P_o(T+10)}{P_o(T)} = \frac{1+\exp\left(\Delta G(T)/k_B T\right)}{1+\exp\left(\Delta G(T+10)/k_B(T+10)\right)}.$$

SUPPLEMENTARY FIGURES

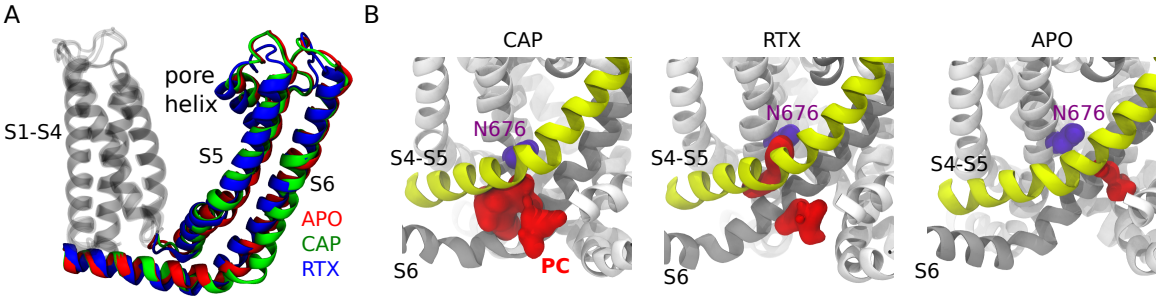

Figure S1: Comparison of the three cryo-EM structures: apo, capsaicin-bound (CAP-bound) and resiniferatoxin-bound (RTX-bound). A. Structural alignment of the three states. The structures were aligned on the S1-S4 domain (transparent, residues 430-557), which does not undergo major conformational rearrangements during gating; the root mean square deviation between any two of these structures is ~ 1 Å if the calculation is restricted to the S1-S4 domain. The pore domain (red, green and blue for apo, CAP-bound and RTX-bound, respectively), on the other hand, is different across the three states. The most striking difference is at the level of the C-terminus of S6. Interestingly, CAP-bound differs from apo and RTX-bound more than these two differ from each other. B. Analysis of peripheral cavities (PCs) in the three structures. The cavities, located between S4-S5 (including S5, yellow) and S6 (grey), are shown as red densities; the N676 residues on S6 are colored in purple. Note that only in CAP-bound, but not in the other two, the peripheral cavity is connected to the intracellular compartment (bottom).

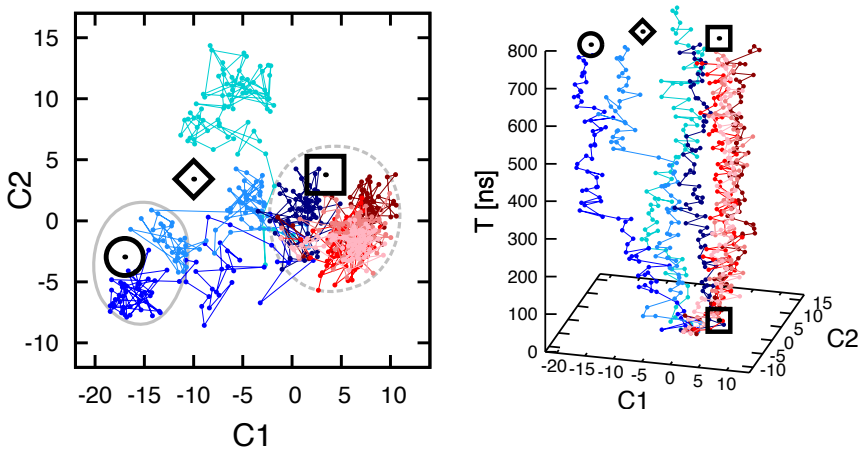

Figure S2: Multidimensional scaling (MDS) analysis of the two MD trajectories of TRPV1 with empty and hydrated PCs. Pairwise distances between structures are based on the overlap between the distance maps (the latter are calculated for the S5 and S6 helices). The diamond, square and circle denote apo, CAP-bound and RTX-bound, respectively. Each of the colored lines corresponds to one subunit of the channel: the lines in blue and red shades correspond to the simulations with empty and hydrated PCs respectively. Note that all four subunits with hydrated PCs fluctuate around the initial state (CAP-bound), while two of the subunits with empty PCs converge to the open structure.

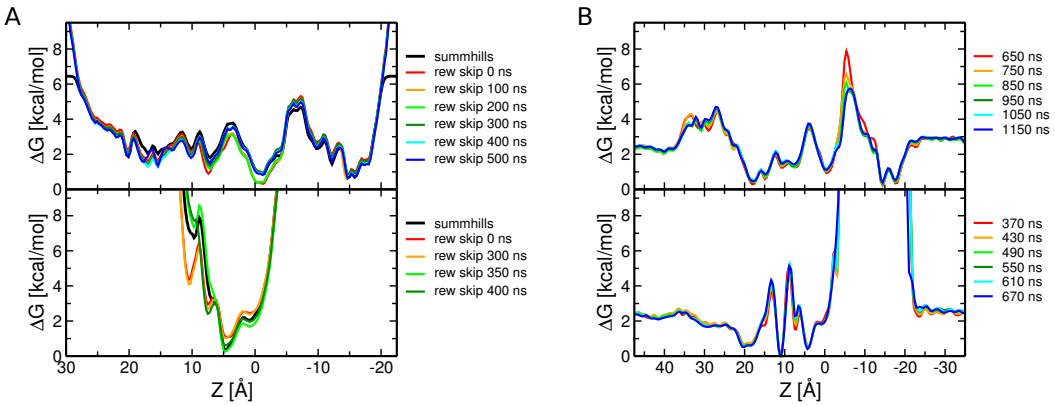

Figure S3: Convergence of the free energy for permeation of a sodium ion through the channel pore. The top and bottom panels correspond to the conformations with empty and hydrated PCs, respectively. A. Free energy profiles generated using the trajectory of a biased ion using either the "sum hills" estimator or the reweighted histograms approach[11]. For the second case, several free energy profiles are shown; for all of them histograms were calculated using only the final part of the trajectory, different colors indicate different initial times for data collection. Note that the two estimators provide consistent free energy profiles. B. Free energy profiles generated from the trajectories of all ions in the system (including the non-biased ones) using the reweighting histogram approach. To assess convergence, we calculated the profiles after regular time intervals. In the case of TRPV1 with empty PCs, the free energy profile does not change significantly after ~ 750 ns (i.e. during last 400 ns). In the case of TRPV1 with hydrated PCs, the free energy profile does not change significantly after ~ 370 ns (i.e. during last 300 ns).

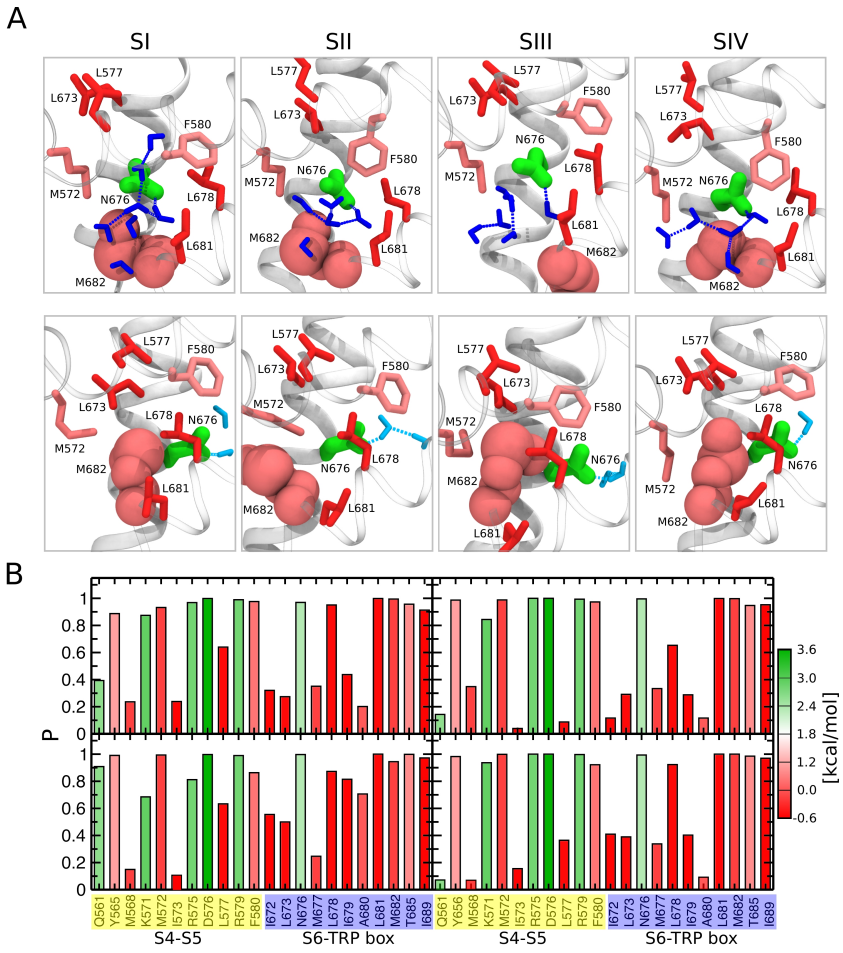

Figure S4: TRPV1 residues exposed to the peripheral cavities. The residues are colored according to their polarity[2] (green is hydrophilic, and red is hydrophobic). A. PCs filled with water (shown in blue, top panel) or empty (bottom panel). The labels SI-SIV denote four TRPV1 subunits. S6 is shown in white, and the S4-S5 linker and the adjacent S6 helix are transparent. Top panel: N676 (shown as sticks) establishes hydrogen bonds with water inside the PC. Except for N676, all the other residues exposed to the PC are hydrophobic. The M682 side chain (space filling representation) located at the entrance to the PC is in a folded conformation. Bottom panel: N676 faces the central pore and interacts with the pore waters (shown in cyan). The M682 side chain is located inside the PC and adopts an extended conformation. B. The probability of being exposed to the PCs (in the channel with hydrated PCs) is shown for the residues in the S4-S5, S6 and TRP-box regions. The four panels correspond to the four TRPV1 subunits. The probabilities are calculated for the last half of the MD trajectory.

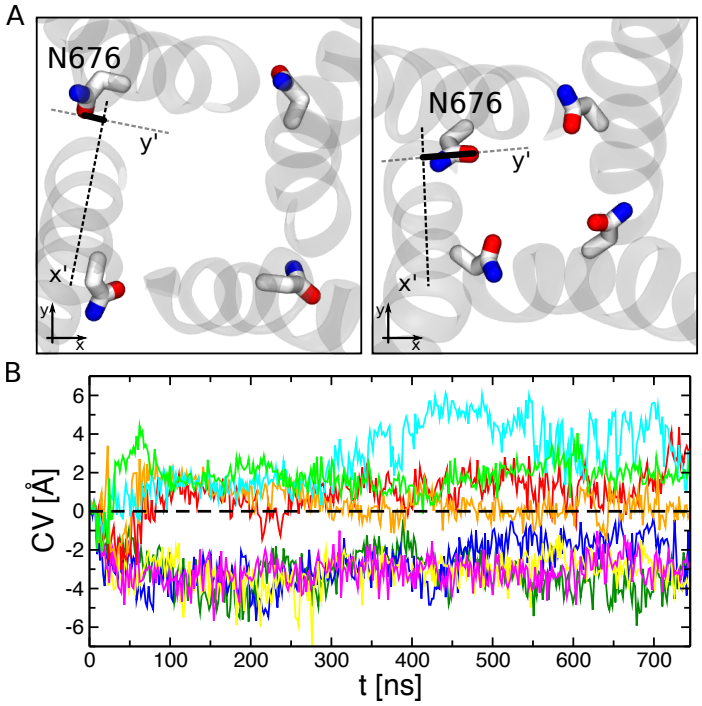

Figure S5: Two distinct N676 orientations in the TRPV1 closed and open states. A. Schematic representation of the collective variable (CV), describing the N676 orientation with respect to the central pore and the adjacent peripheral cavity. The closed and open states are shown on the left and right panels respectively. The S6 helices are shown in grey. The N676 residues are colored by the atom type: C – white, N – blue, and O – red. The CV is the y' coordinate of the N676 side chain carboxamide oxygen (thick black line). B. Evolution of the CV along time estimated for each TRPV1 subunit: with hydrated (red, orange, light-green and cyan) and empty PCs (dark-green, blue, yellow and magenta). The dashed black like highlights the y=0 axis. Note that, for the closed state, the collective variable remains negative for the entire duration of the simulation (N676 is inside the PC). In contrast, for the open state, the value of the CV is positive (N676 is inside the central pore).

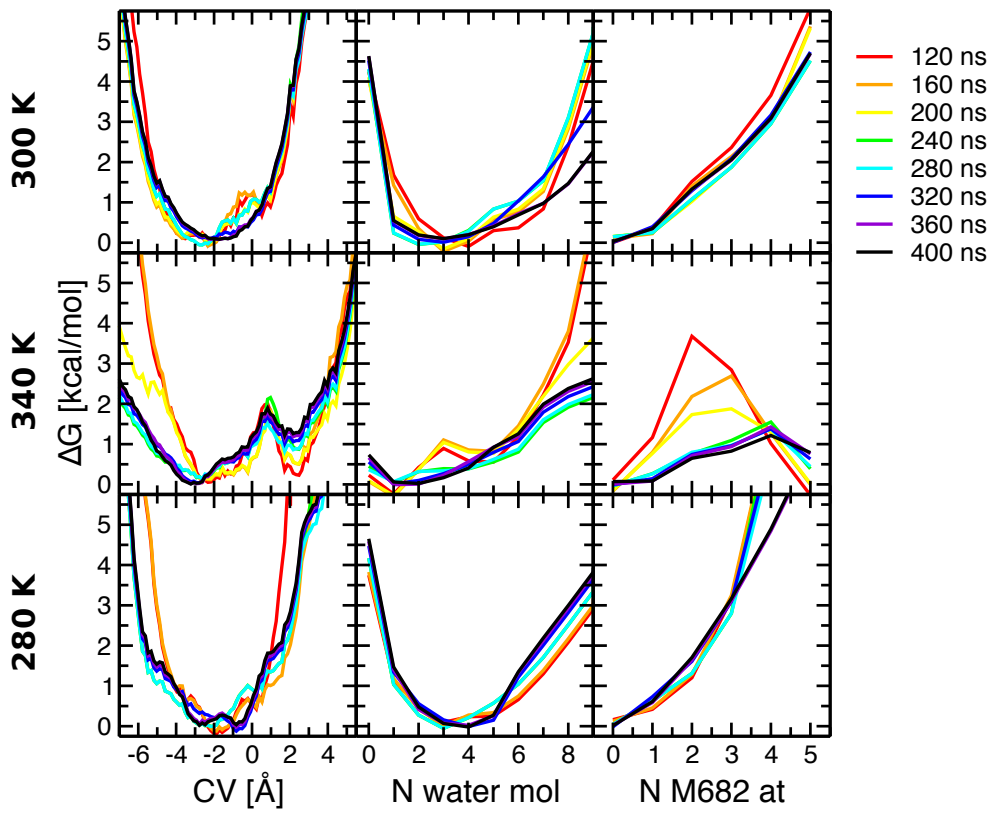

Figure S6: Time evolution of the free energy profiles estimated along the biased CV (N676 rotation with respect to the central pore and the PC, left panels) and the two non-biased degrees of freedom: the number of water molecules and M682 atoms inside the PC (central and right panels, respectively). The top, middle and bottom panels correspond to the simulations at 300, 340 and 280 K. The free energy profiles are estimated with a stride of 40 ns (starting from 120 ns) along the metadynamics runs. Note that all of the free energy profiles do not change significantly after 240 ns, suggesting convergence of the calculation.

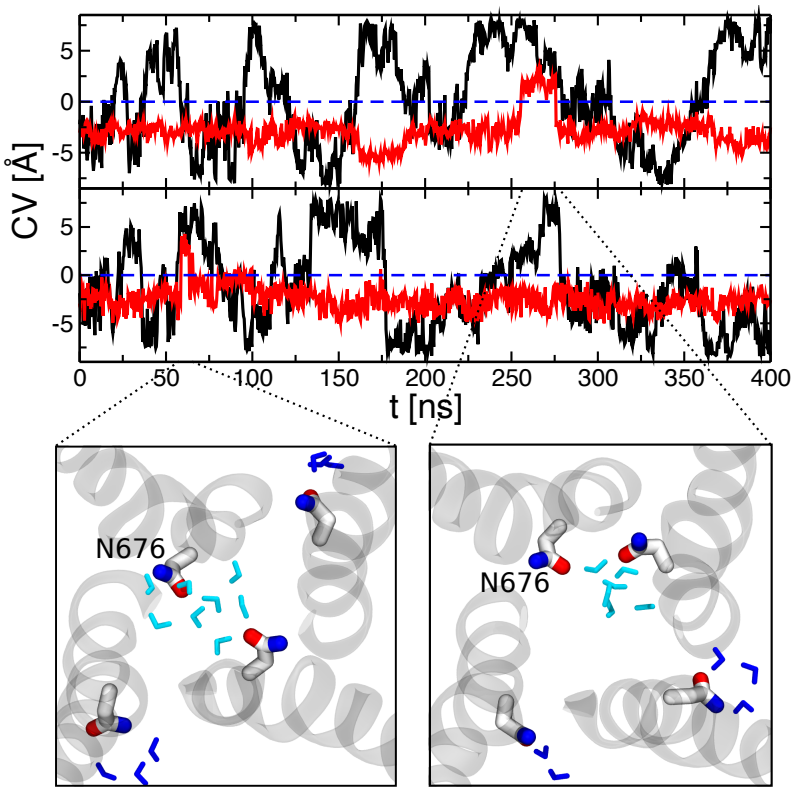

Figure S7: Cooperative effect between the N676 residues of distinct TRPV1 subunits. Top panel: evolution of N676 conformation along the metadynamics runs (at 300 and 340 K – top and bottom rows, respectively). The black and red curves correspond to the biased and non-biased N676 residues, respectively. The dashed blue like highlights the y=0 axis. Bottom panel: cartoon representation of the channel with two N676 (biased and non-biased) facing the central pore. The S6 helices are shown in grey. The N676 residues are colored by atom type: C – white, N – blue, and O – red. Water inside the central pore and the PC is shown in cyan and blue, respectively.

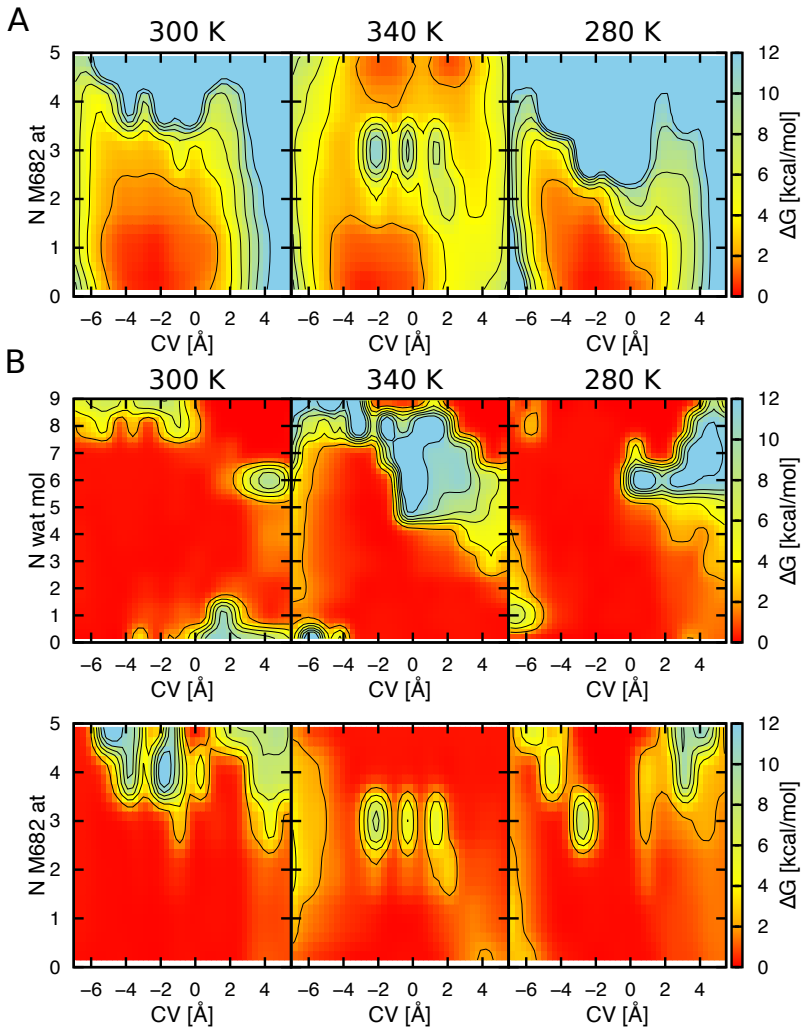

Figure S8: A. Free energy surfaces as a function of the N676 orientation with respect to the central pore (X-axis) and the number of M682 atoms inside the PC (Y-axis). Note that at 340 K, there are two additional thermodynamically stable states compared to the simulations at 300 and 280 K. In these states, the M682 side chain is exposed inside the adjacent PC, while the N676 residue is facing either the PC or the central pore. B. Estimated error on the free energy surfaces. Top and bottom correspond respectively to the “N676 orientation/hydration of the PC” and the “N676 orientation/number of M682 atoms inside the PC” pairs of collective variables. Left, central and right panels correspond to the simulations at 300, 340 and 280 K, respectively.

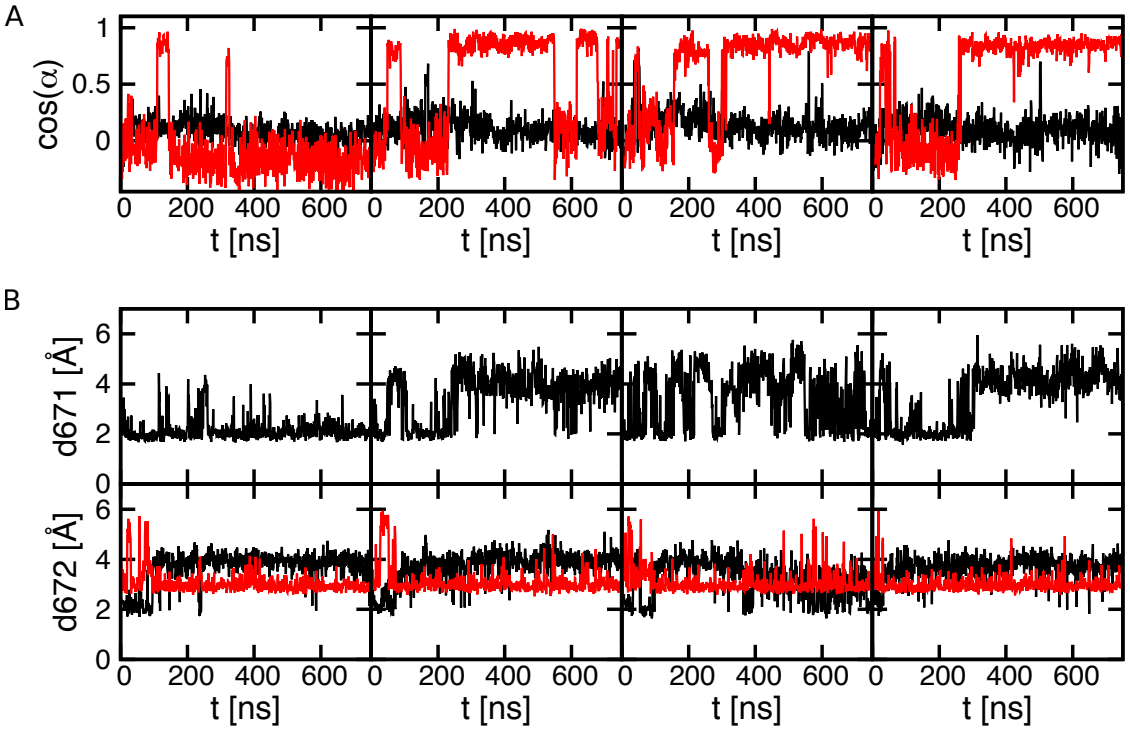

Figure S9: Coupling between the TRPV1 upper and lower gates. The four panels correspond to different TRPV1 subunits A. Orientation of Y671 in the open (black) and closed (red) channel conformations: α is an angle between the side chain of Y671 and the axis of the central pore. Note that in the open and closed states, Y671 is oriented differently: perpendicular or parallel to the central pore, respectively. B. Distance between the carbonyl oxygen of the Y671 backbone and the amino group nitrogen of the L675 backbone in the closed state. Note that disruption of a hydrogen bond between Y671 and L675 (when distance is larger than 2 Å) is correlated with the parallel orientation of the Y671 side chain. B. Distance between the carbonyl oxygen of the I672 backbone and either the amino group nitrogen of the N676 backbone (black) or the carboxamide nitrogen of the N676 side chain (red) in the open state. Note that in each subunit the hydrogen bond between backbone atoms is disrupted after ~ 100 ns. At the same time, I672 establishes a hydrogen bond with the side chain of N676.

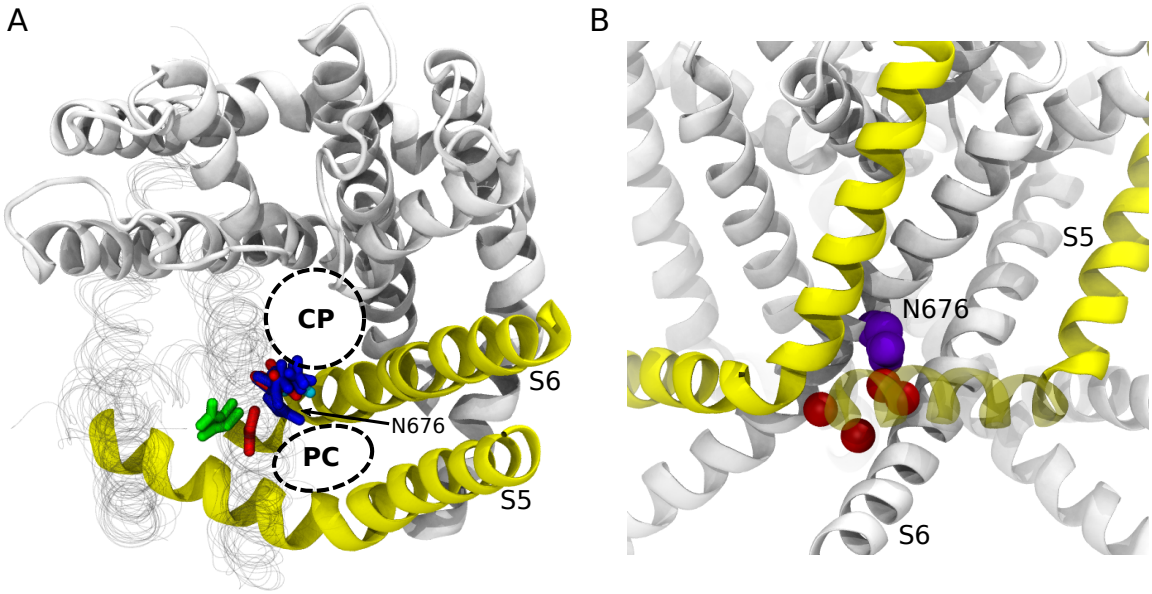

Figure S10: A. Orientation of N676 in different TRP channels, TRPV1 (blue), TRPV2 (green), TRPA1 (cyan) and TRPP2 (red). N676 in the TRPV1 capsaicin-bound structure is highlighted with an arrow. CP and PC correspond to the central pore and the peripheral cavity, respectively. The S5 and S6 helices of the channel subunit adjacent to N676 are colored in yellow. Note that for some channels, such as TRPV1 and TRPP2, both orientations of N676 (inside the central pore or the PC) are captured in different conformational states, while for the others, such as TRPV2 and TRPA1, N676 was shown only in one orientation so far. B. Peripheral cavities in the voltage-gated sodium channel NavMs (pdb code 5HVX[12]). The asparagine residue in the middle of S6 (homologous to N676 in TRPV1) is shown in purple. The structural water interacting with this residue is shown as red spheres.

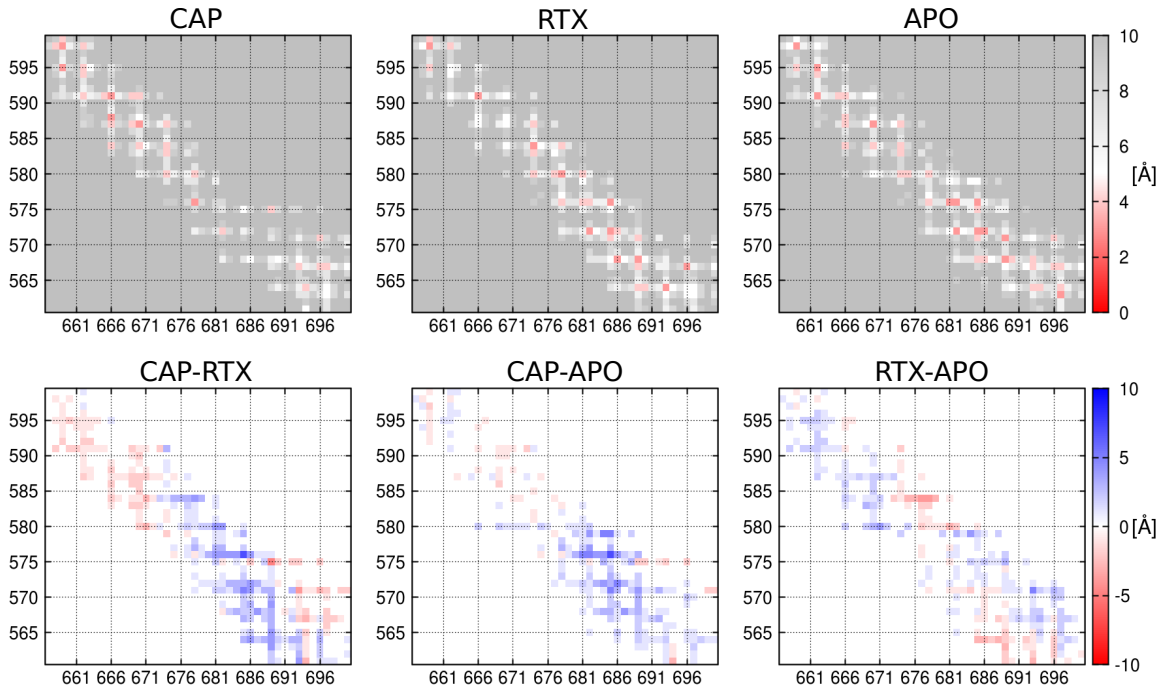

Figure S11: Distance maps calculated for the S4-S5 linker (y-axis) and S6 (x-axis) in the apo, capsaicin-bound (CAP-bound) and resiniferatoxin-bound (RTX) structures (top panel) and the difference between them (bottom panel). The difference between the distance maps indicates that the CAP-bound state is distinct, i.e. it differs from the apo and RTX-bound states more than the latter two differ from each other. The largest difference is at the level of the C-termini interaction surface: in the CAP-bound state, S4-S5 and S6 have significantly less contacts between each other compared to the two other states (a contact is considered to be formed when the corresponding distance is less than 5 Å).

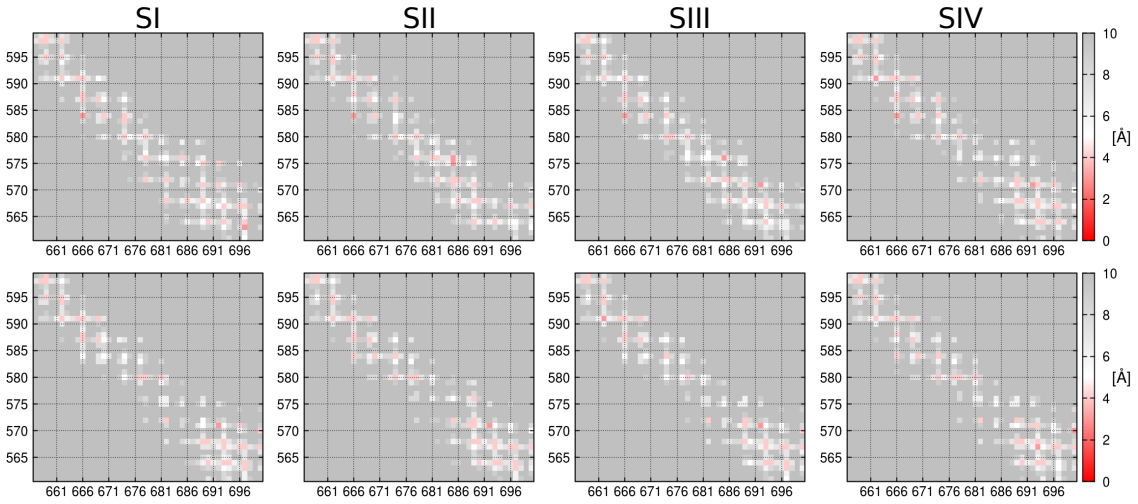

Figure S12: Distance maps calculated for the S4-S5 linker and S6 in the channel conformations with empty (top) or hydrated (bottom) PCs. The SI-SIV labels denote four TRPV1 subunits. Note that in the channel with empty PCs, the C-termini of S4-S5 and S6 form multiple contacts (distance is less than 5 Å) as in the apo or RTX-bound structures. While in the channel with hydrated PCs, the interaction surface between these two structural elements is largely disrupted, similar to the CAP-bound structure.

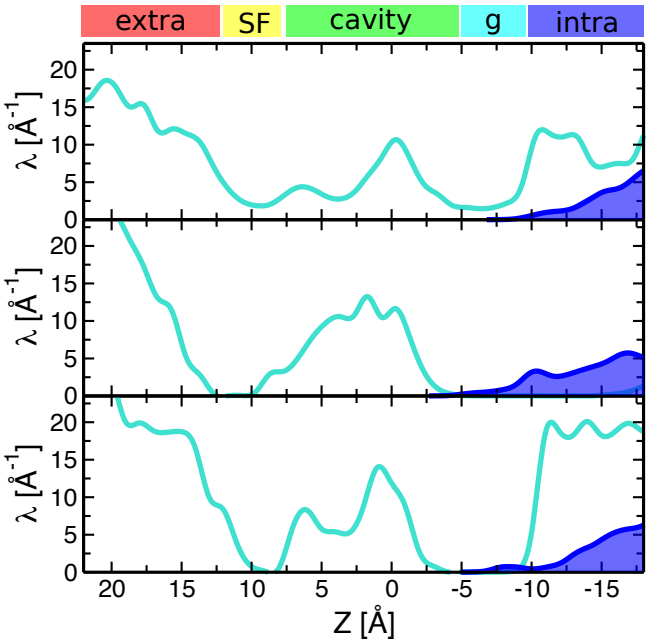

Figure S13: Water density inside the PCs (blue) and the central pore (cyan) in the three TRPV1 states, open (top), closed (middle) and apo (bottom). Z-axis is parallel to the central pore and perpendicular to the membrane plane. Extra, SF, cavity, gate and in denote the extracellular solution, selectivity filter, central cavity, lower gate and intracellular solution. Note that in the closed state, the water density in the PCs extends up to the central cavity; in the apo state, it is nonzero at the level of the lower gate but significantly smaller compared to that of the closed state; and finally, in the open state, the water density in the PCs is interrupted at the level of the lower gate (approximately).

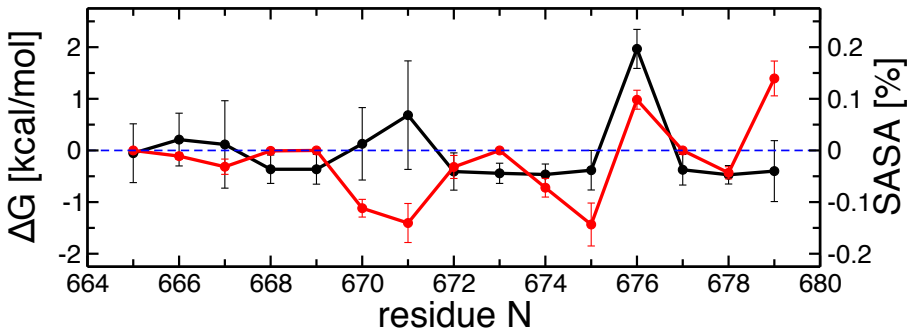

Figure S14: S6 polar properties in the entire TRP family (black curve). The red curve corresponds to the difference in SASA of the S6 residues between the open and closed states and is shown for comparison. Note that the C-terminus residues (positions 672-675, 677 and 678) are markedly hydrophobic for all the family members, while the residue at position 676 is always hydrophilic. The polarity scale was taken from Hessa et al.[2]. The error bars indicate standard deviations.

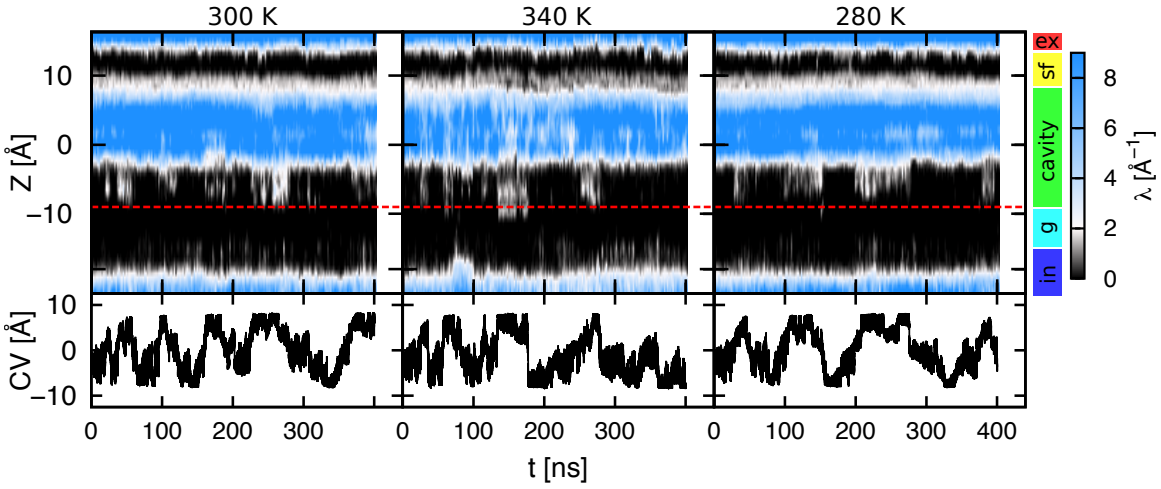

Figure S15: Water density in the central pore at 300 K (top left), 340 K (top center) and 280 K (top right). The red dashed line separates the central cavity from the lower gate. Ex, sf, cavity, gate and in correspond to the extracellular solution, selectivity filter, central cavity, lower gate and intracellular solution, respectively. The dynamics of the N676 orientation with respect to the central pore or the adjacent PC (bottom) is shown for comparison. Note that for all the three simulations, water bursts at the level of the central cavity correlate with positive values of the collective variable, i.e. the conformation with N676 facing the central pore.

SUPPLEMENTARY REFERENCES

1. Liao, M., Cao, E., Julius, D. & Cheng, Y. Structure of the TRPV1 ion channel determined by electron cryo-microscopy. *Nature* **504,** 107–112 (2013).

2. Cao, E., Liao, M., Cheng, Y. & Julius, D. TRPV1 structures in distinct conformations reveal activation mechanisms. *Nature* **504,** 113–118 (2013).

3. Palovcak, E., Delemotte, L., Klein, M. L. & Carnevale, V. Comparative sequence analysis suggests a conserved gating mechanism for TRP channels. *J. Gen. Physiol.* **146,** 37–50 (2015).

4. Hessa, T. *et al.* Recognition of transmembrane helices by the endoplasmic reticulum translocon. *Nature* **433,** 377–381 (2005).

5. Chowdhury, S., Jarecki, B. W., & Chanda, B. A molecular framework for temperature-dependent gating of ion channels. *Cell*, *158*(5), 1148-1158 (2014).

6. Clapham, D. E., Miller, C. A thermodynamic framework for understanding temperature sensing by transient receptor potential (TRP) channels. *Proceedings of the National Academy of Sciences*, **108**(49), 19492-19497 (2011).

7. Vaitheeswaran, S., Yin, H., Rasaiah, J. C., Hummer, G. Water clusters in nonpolar cavities. *Proceedings of the National Academy of Sciences of the United States of America*, **101**(49), 17002-17005 (2004).

8. Wang, L., Zhao, J., Fang, H. Water clusters confined in nonpolar cavities by ab initio calculations. *The Journal of Physical Chemistry C*, **112**(31), 11779-11785 (2008).

9. Nigra, P., Carignano, M. A., Kais, S.. Study of phase changes of the water octamer using parallel tempering and multihistogram methods. *The Journal of Chemical Physics*, **115**(6), 2621-2628 (2001).

10. Jara-Oseguera, A., Bae, C. & Swartz, K. J. An external sodium ion binding site controls allosteric gating in TRPV1 channels. *eLife* **5,** (2016).

11. Tiwary, P., Parrinello, M. A Time-Independent Free Energy Estimator for Metadynamics. *J. Phys. Chem. B* **119,** 736–742 (2015).

12. Sula, A. *et al.* The complete structure of an activated open sodium channel. *Nat. Commun.* **8,** 14205 (2017).